

THE INTERACTION OF ELKS WITH  $Ca^{2+}$  CHANNEL  $\beta$  SUBUNITS  
MAY CONTRIBUTE TO ACTIVE ZONE ORGANIZATION

BY

Sara E. Billings

Submitted to the graduate degree program in Anatomy and Cell Biology and the  
Graduate Faculty of the University of Kansas in partial fulfillment of the  
requirements for the degree of Master of Arts

---

Chairperson Hiroshi Nishimune, Ph.D.

---

Brian Ackley, Ph.D.

---

Dianne Durham, Ph.D.

Date defended: November 17, 2011

The Thesis Committee for Sara Billings  
certifies that this is the approved version of the following thesis:

THE INTERACTION OF ELKS WITH  $Ca^{2+}$  CHANNEL  $\beta$  SUBUNITS  
MAY CONTRIBUTE TO ACTIVE ZONE ORGANIZATION

---

Chairperson Hiroshi Nishimune

Date approved: \_\_\_\_\_

## Abstract

The cytoskeletal matrix of the active zone (CAZ) and synaptic voltage-dependent calcium channels (VDCCs) are both required for the organization and regulation of synaptic vesicle release. Here we report a novel interaction between the CAZ protein family ELKS and VDCC  $\beta$  subunits. We found that two isoforms of ELKS (ELKS2 and ELKS1b) and two isoforms of VDCC  $\beta$  subunits ( $\beta$ 1b and  $\beta$ 4) co-immunoprecipitated. Using fluorescent immunohistochemistry, we observed colocalization between ELKS1b and VDCC  $\beta$ 4 at synapses in the molecular layer of the cerebellum, suggesting a synaptic role for the interaction of these two proteins. Analysis of a P/Q-type VDCC knockout mouse (*Cacna1a*<sup>-/-</sup>) revealed that the localization of the VDCC  $\beta$ 4 subunit to the molecular layer was disrupted, although ELKS1b protein localization was not affected. The results demonstrate that two isoforms of the ELKS family and two VDCC  $\beta$  subunits interact and suggest that their interaction may play a role in the organization of the active zone.

## **Acknowledgements**

I would like to thank Dr. Nishimune for his willingness to share his advice, expertise and experience with me during the past three years. I am grateful to my committee members, Dr. Dianne Durham and Dr. Brian Ackley, for their valuable time and support. To the Nishimune lab members, Jie Chen, Gwenaëlle Clarke and Takafumi Mizushige, thank you all so much for your help, support and encouragement. I would like to thank Ruchira Singh, whose friendship has been immensely valuable, as well as my parents and siblings, for whose support and love I am very, very grateful. I feel incredibly lucky to have such a kind, fun and wonderful family. Most of all, I would like to thank Elvis Huarcaya Najarro, for listening to me during our long walks, believing in me, encouraging me and loving me. Without you, this work would not have been possible.

## Table of Contents

<b>Abstract</b> .....	<b>iii</b>
<b>Acknowledgements</b> .....	<b>iv</b>
<b>List of Figures</b> .....	<b>vi</b>
<b>List of Tables</b> .....	<b>vi</b>
<b>1. Introduction</b> .....	<b>1</b>
<b>2. Methods</b> .....	<b>12</b>
<b>3. Results</b> .....	<b>18</b>
<b>4. Discussion</b> .....	<b>30</b>
<b>5. Conclusions</b> .....	<b>35</b>
<b>6. References</b> .....	<b>36</b>
<b>7. Appendix</b> .....	<b>42</b>

## List of Figures

- Fig. 1.1      Organization of the active zone
- Fig. 1.2      Organization of the cerebellar cortex
- Fig. 1.3      *in situ* hybridization of ELKS1 and VDCC  $\beta$ 4 in cerebellum
- Fig. 3.1      Co-immunoprecipitation of ELKS2 and VDCC  $\beta$ 1b
- Fig. 3.2      Co-immunoprecipitation of ELKS1 and VDCC  $\beta$ 4
- Fig. 3.3      Expression of ELKS1 and VDCC  $\beta$ 4 protein in cerebellum
- Fig. 3.4      Colocalization of ELKS1b/2 and VDCC  $\beta$ 4
- Fig. 3.5      Colocalization of ELKS1b/2 and VDCC  $\beta$ 4 at synapses
- Fig. 3.6      Expression of ELKS1b/2 and VDCC  $\beta$ 4 protein in  
*Cacna1a*<sup>-/-</sup> cerebellum
- Fig. 3.7      Quantification of ELKS1b/2 and VDCC  $\beta$ 4 signal intensity in  
*Cacna1a*<sup>-/-</sup> cerebellum

## List of Tables

- Table 1      ELKS nomenclature

# 1. Introduction

## Study rationale

Synaptic vesicle release results from the influx of calcium through voltage-dependent calcium channels (VDCCs) (Katz, 1996) at highly specialized regions of the presynaptic membrane called active zones (Landis et al., 1988). When calcium enters the presynaptic terminal through a VDCC, the calcium concentration increases steeply in a small domain immediately surrounding the VDCC (Neher, 1998). As it is this increase in calcium concentration that triggers synaptic vesicle release (Katz, 1996), calcium channels, synaptic vesicles and regulatory proteins need to be in close proximity (Stanley, 1997), and are therefore likely to interact. This thesis is primarily concerned with the organization of the active zone and is particularly focused on the interactions between calcium channels and the proteins of the active zone cytomatrix that have structural and regulatory roles at the active zone.

## Calcium channels

VDCCs are central to the process of synaptic transmission. VDCCs consist of the pore-forming  $\alpha$  subunit and auxiliary  $\beta$  and  $\alpha_2\delta$  subunits (Catterall, 2000). The  $\beta$  subunit is an intracellular protein and has a strong affinity for the  $\alpha_1$  subunit (De Waard et al., 1995). The  $\alpha_2\delta$  subunit is an extracellular protein and may have synaptogenic functions that are independent of its participation in the calcium channel complex (Eroglu et al., 2009; Kurshan et al., 2009). A  $\gamma$  subunit

has been proposed to join postsynaptic calcium channel complexes in some systems, but its presence and function is debated (Black, 2003; Leitch et al., 2009).

Of the genes that encode VDCC  $\alpha$  subunits,  $\alpha$ 1A (P/Q-type VDCC,  $Ca_v2.1$ ),  $\alpha$ 1B (N-type VDCC,  $Ca_v2.2$ ) and  $\alpha$ 1E (R-type VDCC,  $Ca_v2.3$ ) are the primary mediators of synaptic transmission (Catterall, 2000). While all four of the VDCC  $\beta$  subunits are able to interact with each VDCC  $\alpha$ 1 subunit (De Waard et al., 1995; Scott et al., 1996; Muller et al., 2010), it appears that some VDCC  $\alpha$ 1 subunits have a preference for specific VDCC  $\beta$  subunits (Muller et al., 2010; Obermair et al., 2010). For instance, the VDCC  $\alpha$ 1A subunit (P/Q-type VDCC) binds most strongly to the VDCC  $\beta$ 4 subunit (De Waard et al., 1995; Muller et al., 2010). The biochemical basis for a preferential interaction between VDCC  $\alpha$ 1A and VDCC  $\beta$ 4 may lie in the fact that, in addition to the high affinity binding site that allows all VDCC  $\beta$  subunits to bind to VDCC  $\alpha$  subunits, VDCC  $\beta$ 4 has two lower affinity interaction sites that increase its specificity to the VDCC  $\alpha$ 1A subunit (Walker et al., 1998; Walker et al., 1999).

### **Calcium channels are important for the integrity of the active zone**

Previous work from our lab demonstrated that the interaction of calcium channels with the extracellular matrix molecule laminin  $\beta$ 2 was necessary for maintenance of active zone structure at the neuromuscular junction (NMJ), as well as able to induce presynaptic differentiation in motor neurons (Nishimune et al., 2004). This suggests that VDCCs play an important role in the organization of

the active zone. The interaction between VDCC  $\beta 4$  and CAZ proteins reported in this thesis is one potential mechanism by which extracellular interactions of VDCCs might influence the organization of the active zone.

### **Cytomatrix of the active zone**

The cytomatrix of the active zone (CAZ) is a densely interlinked network of proteins that overlies the presynaptic membrane (Landis et al., 1988; Schoch and Gundelfinger, 2006). CAZ proteins interact with synaptic vesicles, regulate synaptic vesicle fusion, and most likely specify the location of synaptic vesicle fusion (Rosenmund et al., 2003). Vertebrate active zone proteins include Bassoon, Piccolo, Muncs, RIMs, and the ELKS/CAST/Rab6 interacting protein family (Fig. 1.1) (Schoch and Gundelfinger, 2006). Many interconnections among CAZ proteins have been described, as exemplified by the ELKS/CAST/Rab6 interacting protein family, which links to all known active zone proteins (Schoch and Gundelfinger, 2006; Hida and Ohtsuka, 2010).

### **Links between $\text{Ca}^{2+}$ channels and CAZ**

In contrast to the extensive knowledge about interconnections between CAZ proteins (Schoch and Gundelfinger, 2006), only two of the CAZ proteins, Rim and Piccolo, had been reported to interact with VDCCs when we began these studies (Coppola et al., 2001; Shibasaki et al., 2004; Kiyonaka et al., 2007; Uriu et al., 2010; Kaeser et al., 2011). In *Drosophila* NMJs, it was recently reported that the synaptic calcium channel ( $\alpha 1$  subunit) interacts directly with the

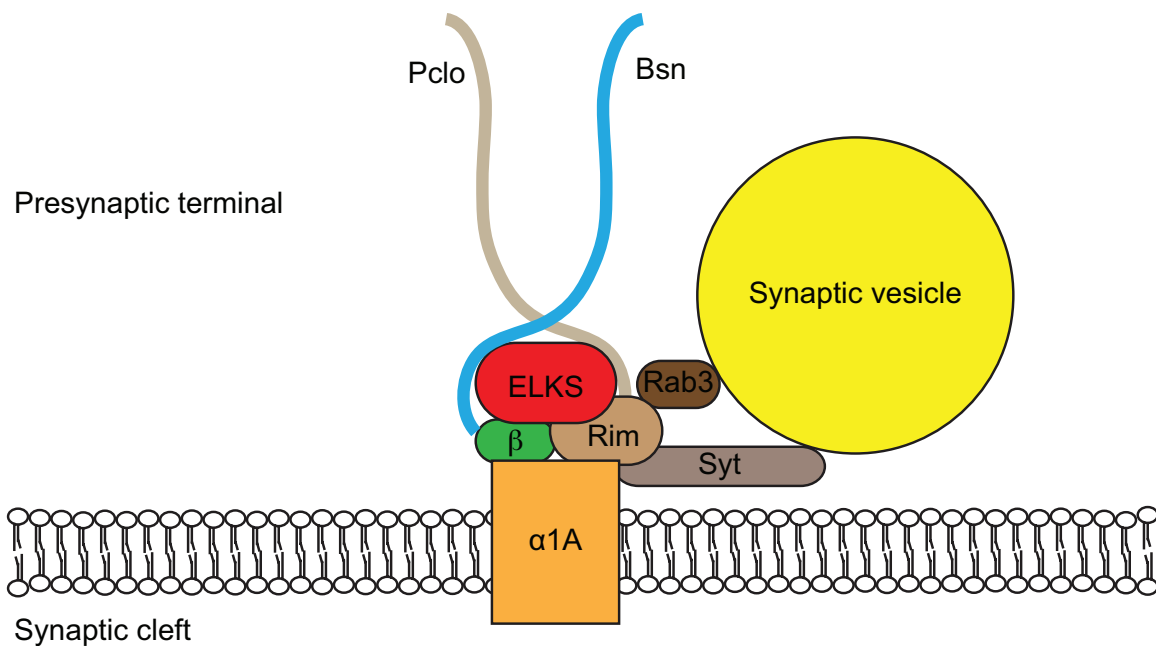


**Figure 1.1 Active zone function requires close association of VDCCs, synaptic vesicles and CAZ proteins like ELKS and Bassoon.** The VDCC  $\alpha 1A$  subunit has a very tight association with the VDCC  $\beta$  subunit, but it also interacts with a wide variety of proteins (Muller et al., 2010). The CAZ proteins (Bassoon, Bsn; Piccolo, Pclo, Rim and ELKS) have so many interconnections amongst themselves that not all interactions could be shown. Synaptotagmin (Syt) and Rab3 proteins link the calcium channel and CAZ complexes to the synaptic vesicles, which is important for efficient neurotransmission. ELKS occupies a central position in the CAZ, as it binds to many of the other active zone proteins.

ELKS family member Bruchpilot (Fouquet et al., 2009). This suggested the possibility that the ELKS family of proteins might bind to VDCCs in vertebrates as well. Indeed, our recent publication demonstrated that vertebrate forms of ELKS2 were capable of interacting with VDCCs through the  $\beta$  subunits (Chen et al., 2011). We also showed that Bassoon could interact with VDCCs (Chen et al., 2011).

### **ELKS proteins**

ELKS proteins are encoded by two separate genes: ELKS1 and ELKS2 (Wang et al., 2002). The nomenclature of these two genes was complicated by multiple independent clonings and characterizations (See Table 1 for summary). ELKS2 was first discovered in a screen for synapse-specific proteins and is very specific to the brain, so its role in the synapse is well characterized (Ohtsuka et al., 2002). It is also present in NMJs (Juraneck et al., 2006).

It appears that both ELKS1 and ELKS2 have multiple splice variants (Kaeser et al., 2009). Alternative splicing of exon 17 creates the best-characterized splice variants of ELKS1, ELKS1a and ELKS1b, which have different C-termini. ELKS1a is a ubiquitous, cytosolic protein that interacts with Rab6 and MICAL3 to promote constitutive vesicle exocytosis and has also been implicated in insulin exocytosis regulation (Ohara-Imaizumi et al., 2005; Grigoriev et al., 2011). The mRNA for ELKS1a can be detected in the brain (Nakata et al., 2002), but its protein expression by western blot is extremely low (Wang et al., 2002; Kaeser et al., 2009). ELKS1b is a brain-specific splice variant that has an

**Table 1 ELKS nomenclature**

<b>Reference</b>	<b>ELKS1a</b>	<b>ELKS1b</b>	<b>ELKS2</b>
(Nakata et al., 2002)	ELKS $\delta$ ELKS $\epsilon$	ELKS $\alpha$ ELKS $\beta$ ELKS $\gamma$	
(Monier et al., 2002)	Rab6IP2B	Rab6IP2A	
(Wang et al., 2002)	Erc1a	Erc1b	Erc2
(Ohtsuka et al., 2002)			CAST
(Deguchi-Tawarada et al., 2004)		CAST2	CAST1
(Kaeser et al., 2009)	ELKS1 $\alpha$ A	ELKS1 $\alpha$ B	ELKS2 $\alpha$ B

identical C-terminus to that of ELKS2 and exhibits similar characteristics to ELKS2 in that it binds to Rim1 and localizes to the active zones (Ohtsuka et al., 2002; Wang et al., 2002; Deguchi-Tawarada et al., 2004; Inoue et al., 2006). Like ELKS2, ELKS1b can be found in the insoluble synaptic fractions when the brain homogenate is subjected to subcellular fractionation, although it is also present in a soluble cytosolic form (Ohtsuka et al., 2002; Wang et al., 2002; Ko et al., 2006). Given these similarities to ELK2, ELKS1b is likely to be important for synaptic function.

However, the exact function of ELKS proteins in the brain is currently unclear. Interruption of Rim1 binding to ELKS and siRNA-mediated knockdown of ELKS1b have been found to decrease  $Ca^{2+}$ -dependent exocytosis in excitatory synapses in cell culture models (Takao-Rikitsu et al., 2004; Inoue et al., 2006), suggesting that ELKS is required for neurotransmission. However, in an ELKS2 knockout mouse, the loss of ELKS2 protein enhanced inhibitory synaptic transmission (Kaeser et al., 2009), indicating that the normal function of ELKS2 is to restrict the amplitude of inhibitory synaptic transmission. It is therefore uncertain whether ELKS proteins positively or negatively regulate neurotransmission. The discrepancy might be resolved by considering that some functions of ELKS proteins may not have been apparent in the ELKS2 knockout mouse due to compensation by the ELKS1b protein. While an ELKS1 knockout has been made (Sudhof, 2008), no detailed report on it exists. According to the preliminary report in the Mouse Genome International database (Sudhof, 2008), the ELKS1 knockout mouse dies at embryonic day 9, consistent with a significant

role for this protein, although it is currently impossible to distinguish the phenotype due to loss of ELKS1b in the brain from that due to the loss of the ubiquitous ELKS1a isoform.

## **Cerebellum**

The cerebellar cortex has three layers: the molecular, Purkinje cell and granule cell layers (Fig. 1.2). Granule cells send their axons (called parallel fibers) up into the molecular layer, where they bifurcate and run parallel to the cerebellum lobules (Palay and Chan-Palay, 1974). In this study we will use parasagittal sections of the cerebellum, so that the parallel fibers are cross-sectioned and have a puncta-like appearance in the molecular layer. The parallel fibers form synapses with Purkinje cell dendrites that are called parallel fiber-Purkinje cell synapses. These glutamatergic, excitatory synapses are the predominant synapse type in the molecular layer (Palay and Chan-Palay, 1974).

ELKS1b is highly expressed in the granule cells of the cerebellum, where there is little to no ELKS2 expression (Ko et al., 2006; Kaeser et al., 2009). VDCC  $\beta$ 4 is the most highly expressed  $\beta$  subunit in the cerebellum (Ludwig et al., 1997). The expression pattern of ELKS1 and VDCC  $\beta$ 4 can be seen in Figure 1.3. The strongest expression of ELKS1 is in the granule cells, whereas VDCC  $\beta$ 4 is expressed in both the granule cells and the Purkinje cells (Fig. 1.3). The high expression of ELKS1b and VDCC  $\beta$ 4 combined with the low expression of ELKS2 makes the cerebellum an ideal place to probe a potential interaction between ELKS1b and VDCC  $\beta$ 4. Therefore, we chose the cerebellum as a model

system to analyze the interaction between ELKS1b and VDCC  $\beta$ 4 to determine whether they might connect the CAZ complex to VDCCs and contribute to active zone organization.

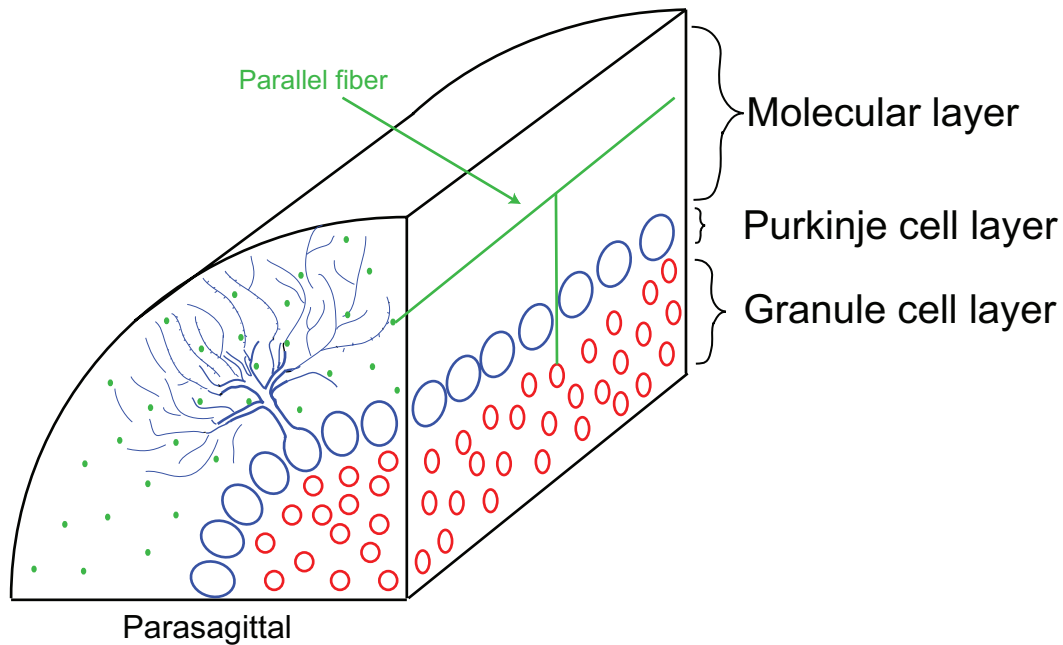


**Figure 1.2 The cerebellar cortex contains three well-defined layers.** The exterior molecular layer contains parallel fiber-Purkinje cells synapses. The dendrites of the Purkinje cells fan out in the parasagittal plane in the molecular layer, and the Purkinje cell bodies (blue) form a monolayer just below. The granule cell bodies (red) pack densely in the third layer. The parallel fibers (granule cell axons, green) extend from the granule cell bodies into the molecular layer, run parallel to the parlobular plane, and synapse with the Purkinje cell dendrites (blue). For clarity, the processes of only one Purkinje and one granule cell were elaborated.

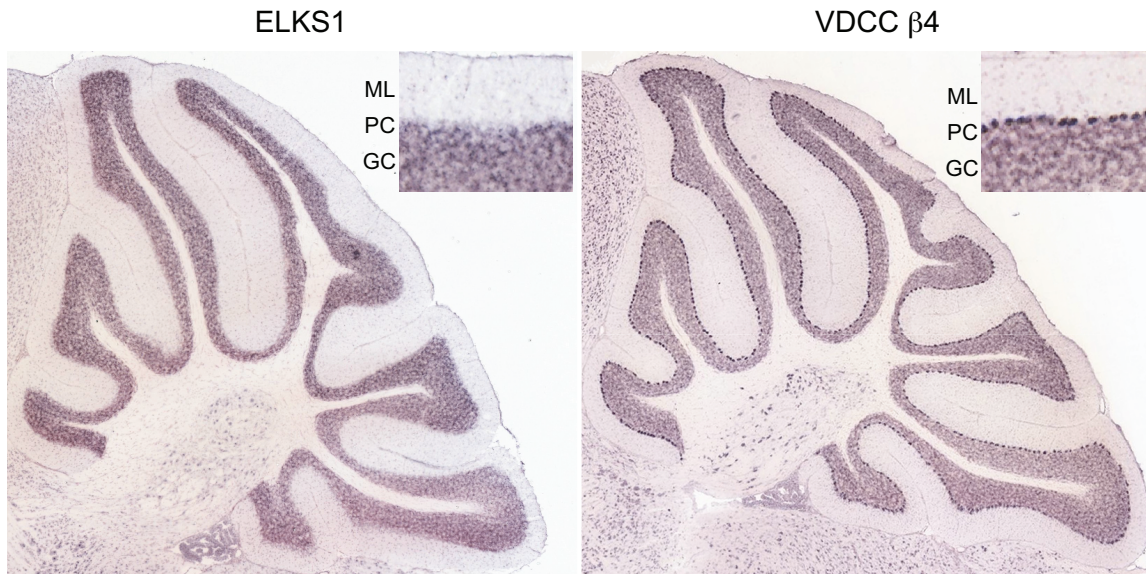


**Figure 1.3 Expression of ELKS1 and VDCC  $\beta$ 4 mRNA in cerebellum.** *In situ* hybridization was performed on sagittal cerebellar sections using probes specific for ELKS1 and VDCC  $\beta$ 4. Both ELKS1 and VDCC  $\beta$ 4 are highly expressed in the granule cells (GC), which send axons up into the molecular layer (ML) to synapse with Purkinje cell (PC) dendrites. VDCC  $\beta$ 4, but not ELKS1, is expressed in the PC. Data is from the Allen Brain Atlas at [www.brain-map.org](http://www.brain-map.org).

## 2. Methods

### Animals

*Cacna1a*<sup>-/-</sup> mice on a C57BL6/J background were previously generated and analyzed by Jun and colleagues (1996). All animal procedures were performed in accordance with the regulations of the University of Kansas Medical Center.

### Plasmids

Full-length Flag-ELKS1b was subcloned from the cDNA KIAA 1081 (Kazusa DNA research Institute, Kisarazu, Chiba, Japan) and expressed as a Flag-tagged fusion protein. Full-length Flag-ELKS2 was subcloned from the Image clone 6331997 (Open Biosystems) and expressed as a Flag-tagged fusion protein. The expression plasmid for full-length VDCC  $\beta$ 4 was obtained from Origene (Catalog #: MC201619; Rockville, MD). The pMT2 expression plasmid for VDCC  $\beta$ 1b (rat *Cacnb1*; NM\_145121) was a kind gift from Dr. W. A. Catterall. The expression plasmid for the C-terminal end of VDCC  $\alpha$ 1A (5290-6636 bp) was subcloned from full-length VDCC  $\alpha$ 1A and expressed as a myc-tagged fusion protein.

### Antibodies

The antibodies used in this study were as follows: mouse anti-VDCC  $\beta$ 4 (Neuromab, Davis, CA), mouse anti- $\beta$ 1 (Neuromab, Davis, CA), rabbit anti-ELKS1b/2 (anti-Erc1b/2, Synaptic Systems, Göttingen, Germany), mouse anti-Flag (Sigma, St. Louis, MO), mouse anti-Bassoon (SAP7F407, Enzo Life

Sciences, Plymouth Meeting, PA). Goat secondary antibodies conjugated to Alexa Fluor 488, 568 and 647 were used for fluorescent immunohistochemistry (Invitrogen). Alkaline phosphatase-conjugated secondary antibodies (Jackson ImmunoResearch Laboratories, Inc., West Grove, PA) were used for western blot detection.

### **Co-immunoprecipitation**

HEK293T cells were cultured in DMEM (Sigma), 10% FBS (Sigma) and 2.5% Penicillin/Streptomycin (Invitrogen) at 37°C, in 5% CO<sub>2</sub>. Cells were transfected with the expression plasmids using the calcium-phosphate precipitation method. Cells were harvested after 48-72 hours and lysed by pipetting in Triton-X 100 lysis buffer (150 mM NaCl, 0.5 mM EDTA, 1 mM DTT, 1% vol/vol Triton-X 100, protease inhibitor tablet (Roche), 20 mM Tris, pH 7.4). After rocking for 30 minutes at 4°C, lysate was centrifuged at 10 000xg for 20 minutes. The supernatant containing the heterologously expressed proteins was used in immunoprecipitation reactions.

All incubations took place at 4°C while continually shaking at 1200 rpm in a Fisher Thermomixer. For the immunoprecipitation, the VDCC β- and Flag-ELKS-containing lysates were mixed together in the indicated combinations and incubated for 2 hours. Anti-VDCC β1b or anti-VDCC β4 antibody (0.5 μg) was added to the protein mixture and incubated for one hour. Protein-G-conjugated magnetic beads (Invitrogen) were then added and incubated for one more hour. For the Flag-ELKS1b-VDCC β4 reverse immunoprecipitation, Flag-ELKS1b was

mixed with anti-Flag antibody (0.5 µg) and protein G-conjugated magnetic beads, and then incubated for two hours. The beads, now complexed with anti-Flag antibody and Flag-ELKS1, were isolated from the supernatant, and incubated with VDCC β4 lysate for an additional two hours. After the immunoprecipitation incubations, the beads were washed extensively in Triton-X lysis buffer without the protease inhibitor, boiled in SDS-PAGE buffer, run on either a 7.5 or 10% SDS-PAGE gel, and blotted onto PVDF membranes using standard protocols. Membranes were blocked in 1% BSA/TBS-0.1% Tween 20, incubated with the indicated primary antibodies overnight at 4°C, washed with TBS-0.1% Tween 20, incubated with alkaline phosphatase-conjugated anti-mouse antibody, washed, and developed using CDP-STAR (PerkinElmer, Boston, MA).

### **Immunohistochemistry**

Three pairs of wild-type and *Cacna1a*<sup>-/-</sup> littermates were euthanized at postnatal day 19 with isoflurane (Abbot # 5260-04-05) and perfused with 10 ml phosphate-buffered saline (PBS) followed by 10 ml of 4% paraformaldehyde (PFA) in PBS. Brains were removed and fixed in 4% PFA at room temperature for one hour, and then washed three times in PBS. Tissue was cryoprotected in 20% sucrose/PBS overnight at 4°C and embedded in Tissue Tek Optimal Cutting Temperature medium (Sakura Finetek USA Inc. #4583 Torrance, CA). Twenty-µm-thick sections were cryosectioned and mounted onto Superfrost plus slides (Fisher). Sections were air-dried at room temperature for 10 minutes, rehydrated in PBS for 10 minutes and then blocked for one hour at room temperature in

blocking solution (2% bovine serum albumin (Sigma), 2% normal goat serum (GIBCO), 0.1% Triton X-100 (Sigma) in PBS). The sections were incubated overnight at 4°C with primary antibodies diluted in blocking solution. Sections were washed three times in PBS, incubated with secondary antibodies and 4,6-diamidino-2-phenylindole (DAPI), washed again in PBS and mounted in Vectashield (Vector Laboratories, Burlingame CA). Epifluorescent images were obtained on a Nikon 80i microscope [Plan Fluor 4x lens, NA = 0.13] to evaluate overall staining pattern.

### **Image acquisition for colocalization**

Single optical planes were obtained from the molecular layer of the cerebellum of three wild-type animals using a Nikon C1Si confocal microscope with a 100x APO TIRF lens (Numerical aperture = 1.49). The xy pixel size was 69.1 nm per pixel. Images were exported as 8-bit tiff files and evaluated for colocalization in ImageJ.

### **Colocalization analysis**

An iterative thresholding method was adapted to identify puncta and perform colocalization analyses (Fish et al., 2008). In ImageJ, confocal images were thresholded using the automatic threshold function. Using the Analyze Particle function, puncta of a restricted size range were identified at each of the threshold levels between 255 and the automatic threshold grayscale value. The puncta size range was restricted to between 0.095  $\mu\text{m}^2$  and 0.285  $\mu\text{m}^2$  for the following

reasons: The lower value represents the area of a circle with the diameter of the average active zone length of adult mouse cerebellar parallel fiber-Purkinje cell synapses ( $0.348 \pm 12 \mu\text{m}$ ) (Takeuchi et al., 2005). This size is used as the lower bound because synaptic proteins tend to be evenly distributed along the active zone (Tao-Cheng, 2007), so puncta of synaptic antigens should have a diameter that is close to the full extent of the active zone. The upper value ( $0.285 \mu\text{m}^2$ ) represents the size below which ninety-five percent of synaptic puncta will fall when imaged by light microscopy (Mishchenko, 2010).

The regions of interest (ROI) generated by this process were combined using the ROI manager function and a mask of the combined ROI was created, such that each puncta identified was represented by a particle on the mask. The overlapping area between ELKS1b and VDCC  $\beta 4$  was analyzed by dividing the area of colocalized signals by the total area of ELKS1b signal. The number of colocalizing puncta, which we called ELKS1b-VDCC  $\beta 4$  areas, was analyzed by counting the number of ELKS1b puncta that overlapped with at least  $0.05 \mu\text{m}^2$  or  $0.023 \mu\text{m}^2$  of the VDCC  $\beta 4$  puncta and dividing that number by the total number of ELKS1b puncta.

The percentage of ELKS1b-VDCC  $\beta 4$  areas that overlapped with the active zone marker Bassoon was also calculated to determine whether ELKS1b and VDCC  $\beta 4$  colocalize at synapses. For this, the mask of colocalized areas between ELKS1b and VDCC  $\beta 4$  was size-restricted to greater than  $0.05 \mu\text{m}^2$  using the Analyze Particles function, resulting in a mask of all the ELKS1b-VDCC  $\beta 4$  areas that were larger than  $0.05 \mu\text{m}^2$ . Then, this mask was compared to a

mask of Bassoon signal using the object-based method of colocalization in the JaCOP plugin (Bolte and Cordelieres, 2006). This program found the centers of the ELKS1b-VDCC  $\beta$ 4 areas and then determined whether those centers were located within a Bassoon puncta, which was defined as colocalization. The percentage of ELKS1b-VDCC  $\beta$ 4 areas that colocalized with Bassoon was then calculated by dividing the number of ELKS1b-VDCC  $\beta$ 4 areas colocalizing with Bassoon by the total number of ELKS1b-VDCC  $\beta$ 4 areas.

### **Fluorescent intensity quantification**

Epifluorescent images were obtained on a Nikon 80i microscope [Plan Apo 20x lens, NA = 0.75]. Three pairs of wild-type and knockout littermates were evaluated, and similar areas were imaged for each pair. Four to five areas of the cerebellar cortex were imaged, measured and averaged for each animal. The mean fluorescent intensity of the molecular layer was measured in ImageJ using a box of fixed width (230 pixels) that extended from the pia to the tops of the Purkinje cells. The mean fluorescent intensity of the granule cell layer was measured using a box of 230 pixels squared.

### **Statistics**

We used a paired t-test when comparing wild-type and *Cacna1a*<sup>-/-</sup>, because the animals were littermates and were prepared and analyzed in pairs. Data are reported as mean  $\pm$  SEM.

### 3. Results

#### ELKS proteins bind to VDCC $\beta$ subunits

Our initial set of experiments was performed using the mouse NMJ as a model system (Chen et al., 2011). Therefore, we tested the binding of ELKS2 and VDCC  $\beta$ 1b, because these two proteins are expressed in motor neurons (Pagani et al., 2004; Juranek et al., 2006). Performing co-immunoprecipitation with heterologously expressed protein lysates, we found that ELKS2 bound to  $\beta$ 1b, but not to the C-terminus of VDCC  $\alpha$ 1A (Fig. 3.1A, B)(Chen et al., 2011). We did not observe co-immunoprecipitation in the control reactions when the bait protein was omitted (Fig. 3.1A, B)(Chen et al., 2011). This result shows that ELKS2 and VDCC  $\beta$ 1b form a protein complex *in vitro*.

Next, we tested the binding of ELKS1b and VDCC  $\beta$ 4, which are highly expressed in cerebellum. We found that Flag-ELKS1b protein co-immunoprecipitated with VDCC  $\beta$ 4 (Fig. 3.2A)(Billings et al., 2012). To confirm the specificity of this interaction, we performed the co-immunoprecipitation in reverse, using an anti-Flag antibody against the Flag-ELKS1b protein. We detected co-immunoprecipitation of VDCC  $\beta$ 4, which was the same molecular weight as the input VDCC  $\beta$ 4 band (Fig. 3.2B)(Billings et al., 2012). We did not observe co-immunoprecipitation in the control reactions when the bait protein was omitted (Fig. 3.2A and 3.2B; HEK)(Billings et al., 2012). These data indicated that ELKS1b and VDCC  $\beta$ 4 form a protein complex *in vitro*.

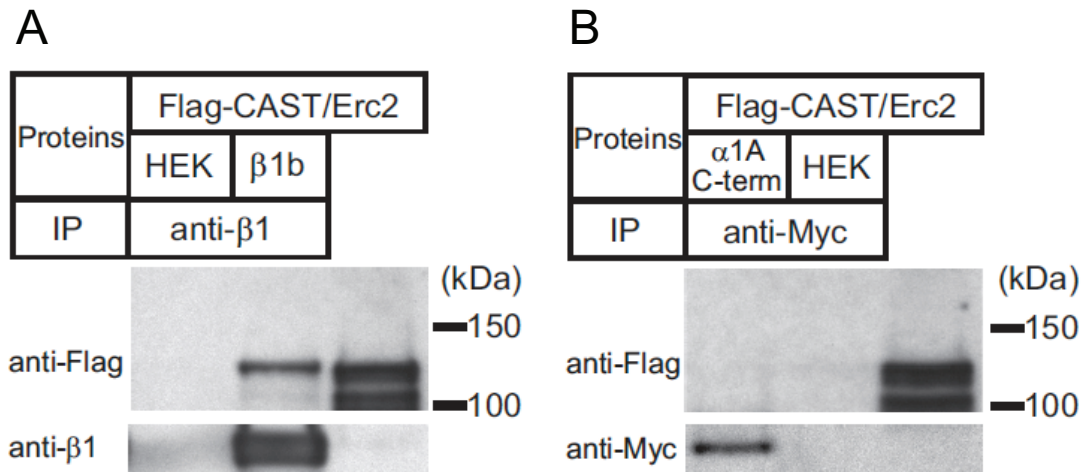


**Figure 3.1 VDCC β1b and ELKS2 form a protein complex.** HEK cell lysates containing heterologously expressed proteins were incubated together in the indicated combinations and then immunoprecipitated with either anti-VDCC β1b or anti-myc antibody. **A**, ELKS2 co-immunoprecipitated with the VDCC β1b subunit. **B**, The Myc-tagged C-terminal cytosolic domain of the α1A subunit did not bind to ELKS2. Input controls (right lanes of each panel) indicate expected molecular weights. Figure adapted from (Chen et al., 2011).

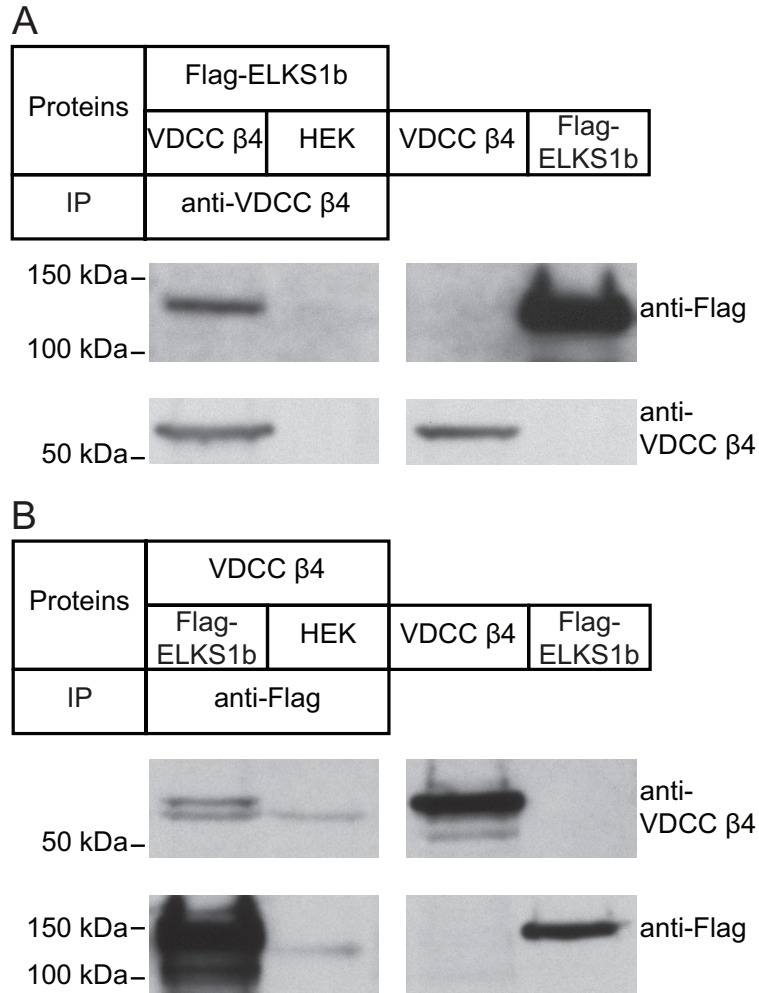


**Figure 3.2 VDCC  $\beta$ 4 and ELKS1b form a protein complex.** HEK cell lysates containing heterologously expressed proteins were incubated together and then immunoprecipitated with either anti-VDCC  $\beta$ 4 or anti-Flag antibody. **A**, Flag-ELKS1b co-immunoprecipitated with VDCC  $\beta$ 4 when an anti-VDCC  $\beta$ 4 antibody was used. **B**, In the reverse co-immunoprecipitation, VDCC  $\beta$ 4 co-immunoprecipitated with Flag-ELKS1b when an anti-Flag antibody was used. The lower molecular weight band observed in both lanes is a non-specific detection of the immunoprecipitation antibody. Input controls (right panels) indicate expected molecular weights. Figure adapted from (Billings et al., 2012).

Taken together, these results demonstrate that both ELKS family members are able to interact with a VDCC  $\beta$  subunit.

### **ELKS1b and VDCC $\beta$ 4 colocalize at molecular layer synapses**

To further investigate the interaction of ELKS1b and VDCC  $\beta$ 4 *in vivo*, we performed immunohistochemistry ELKS1 and VDCC  $\beta$ 4 on sagittal mouse cerebellar sections. Consistent with previous work (Ludwig et al., 1997; Deguchi-Tawarada et al., 2004), ELKS1b/2 and VDCC  $\beta$ 4 antibodies both stained the molecular layer. The ELKS1b/2 antibody recognizes the shared C-terminus of ELKS1b and ELKS2. As ELKS1 is highly expressed in the cerebellum, whereas ELKS2 is below the western blot detection level (Kaeser et al., 2009), the majority of signal observed here is likely to represent ELKS1b staining. While VDCC  $\beta$ 4 staining was highly concentrated in the molecular layer, ELKS1b/2 staining was found at similar intensities in both the molecular layer and the granule cell layer (Fig. 3.3).

We then acquired confocal images of the molecular layer to analyze colocalization. VDCC  $\beta$ 4 and ELKS1b/2 staining revealed many small, closely packed puncta distributed throughout the molecular layer (Fig. 3.4A, B)(Billings et al., 2012), which is consistent with the distribution of synapses between granule cells and Purkinje cells (Palay and Chan-Palay, 1974). We created masks that demarcated the puncta for each antigen (Fig. 3.4D, E)(Billings et al., 2012).

When the overlapping area was analyzed,

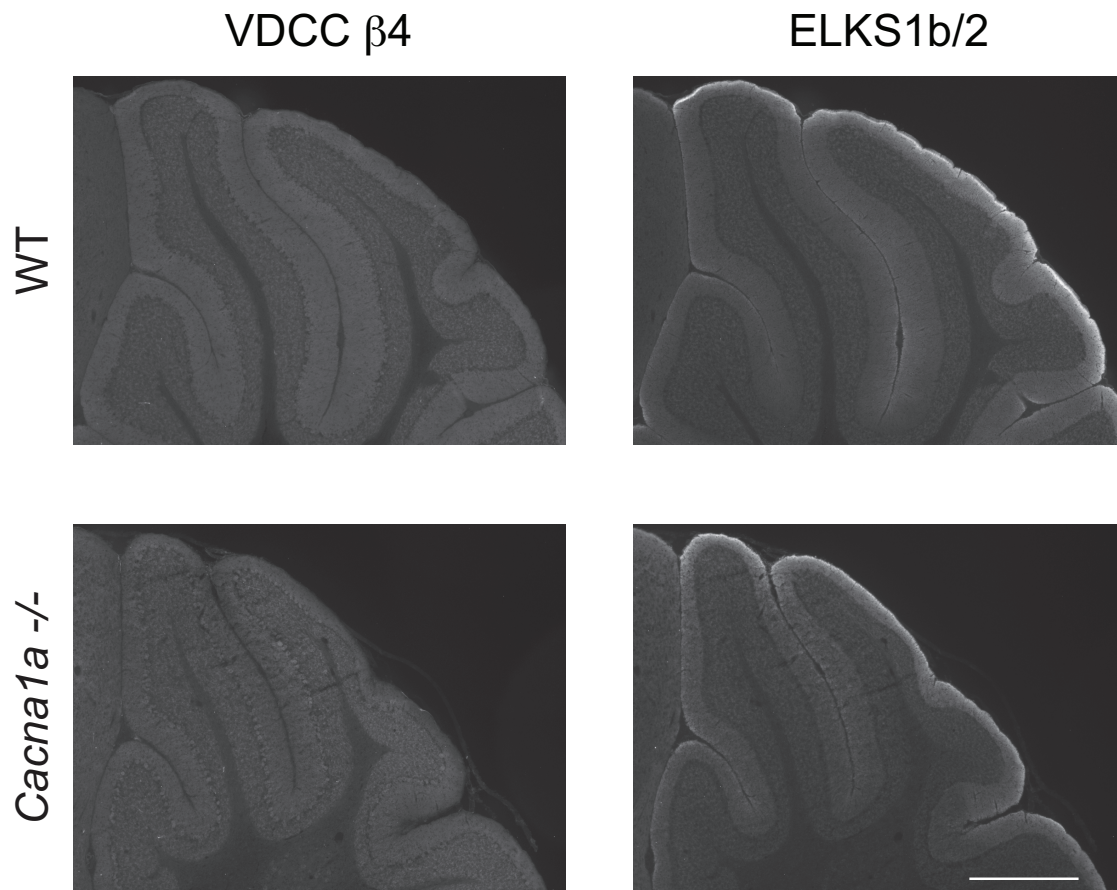


**Figure 3.3 ELKS1b/2 and VDCC β4 protein expression pattern in the cerebellum.** Sagittal sections of wild-type (WT) and *Cacna1a*<sup>-/-</sup> cerebella were stained with anti-VDCC β4 and anti-ELKS1b/2 antibodies and visualized by fluorescent secondary antibodies. Scale bar = 0.5mm

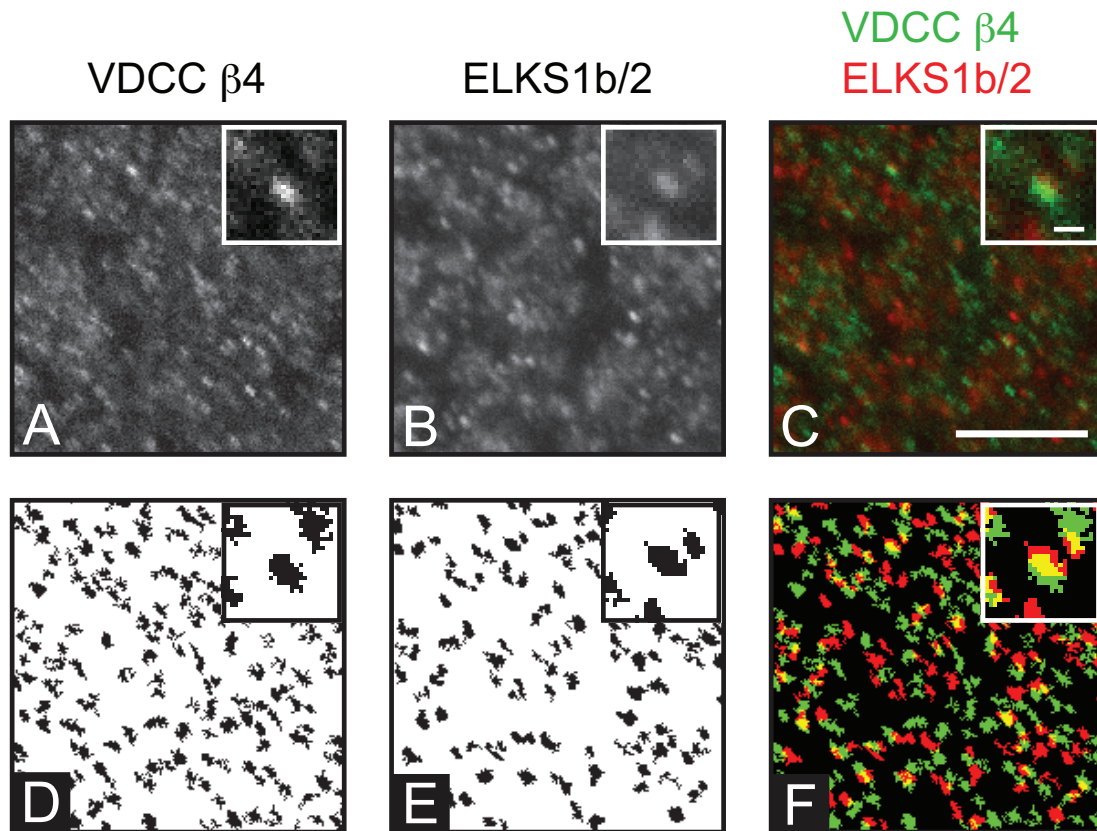


**Figure 3.4** VDCC  $\beta$ 4 and ELKS1b/2 colocalize in the molecular layer of the cerebellum. Single optical planes were acquired by confocal microscopy after fluorescent immunohistochemistry with antibodies against VDCC  $\beta$ 4 and ELKS1b/2 (**A**, **B**), and iterative threshold masks of the puncta for each image were created (**D**, **E**). The merged image (**C**) and mask (**F**) show VDCC  $\beta$ 4 in green and ELKS1b/2 in red and their colocalization in yellow. Scale bar = 5  $\mu$ m. Insets show a magnified area of the images. Scale bar = 500 nm. Figure adapted from (Billings et al., 2012).

16.35 ± 1.06% of the ELKS1b/2 signal overlapped with the VDCC β4 signal (Billings et al., 2012). When the number of colocalizing puncta was analyzed, 25.06 ± 0.89% of the ELKS1b/2 puncta overlapped with VDCC β4 puncta by at least 0.05 μm<sup>2</sup>, and 45.48 ± 1.45% overlapped by at least 0.023 μm<sup>2</sup> (Billings et al., 2012). These results revealed a moderate overlap between VDCC β4 and ELKS1b/2 in the molecular layer and suggested that ELKS1b/2 and VDCC β4 puncta are often found in close proximity to each other.

To determine whether ELKS1b/2 and VDCC β4 puncta overlap at synapses, we co-stained with Bassoon antibody. Bassoon has been widely used as a CAZ marker due to its specific localization to the active zone (Tao-Cheng, 2007) and the fact that it arrives at synapses very early during synaptogenesis (Zhai et al., 2000). Figure 3.5 shows an example of a Bassoon punctum that overlaps with both ELKS1b/2 and VDCC β4. To calculate the number of colocalized ELKS1b/2 and VDCC β4 puncta that overlap with Bassoon, we first created a mask of the areas that colocalized by at least 10 pixels (0.05 μm<sup>2</sup>) between ELKS1b/2 and VDCC β4, which we termed ELKS1b/2-VDCC β4 areas. Then, we calculated the number of these ELKS1b/2-VDCC β4 areas that overlapped with Bassoon signal. We observed that 33.81 ± 3.2% percent of colocalized areas between ELKS1b/2 and VDCC β4 overlapped with Bassoon signal. These data suggest that ELKS1b/2 and VDCC β4 colocalize at molecular layer synapses.

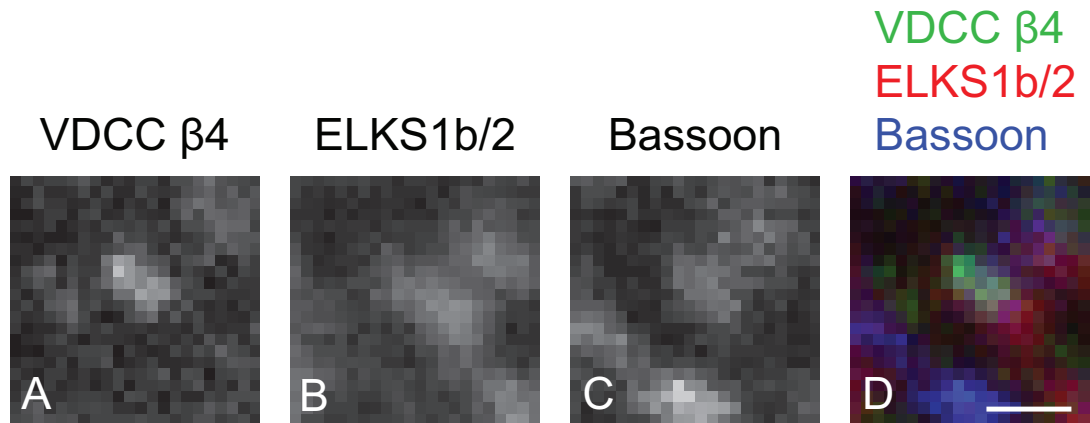


**Figure 3.5 VDCC  $\beta$ 4 and ELKS1b/2 colocalize at Bassoon-marked synapses.** Single optical planes were acquired by confocal microscopy after fluorescent immunohistochemistry with antibodies against VDCC  $\beta$ 4, ELKS1b/2 and Bassoon (**A-C**). The merged image (**D**) shows VDCC  $\beta$ 4 in green, ELKS1b/2 in red, Bassoon in blue and their colocalization in yellow. Thirty-four percent of colocalized VDCC  $\beta$ 4 and ELKS1 areas greater than 10 pixels ( $0.05 \mu\text{m}^2$ ) in size colocalized with Bassoon puncta. Scale bar = 500 nm.

## **VDCC $\beta$ 4 but not ELKS1b localization is disrupted in *Cacna1a*<sup>-/-</sup> cerebellum**

VDCC  $\beta$ 4 is the preferred VDCC  $\beta$  subunit of VDCC  $\alpha$ 1A ( $\text{Ca}_v2.1$ ) (Muller et al., 2010), which forms the P/Q-type VDCC (Catterall, 2000). We hypothesized that the loss of VDCC  $\alpha$ 1A would perturb the localization of VDCC  $\beta$ 4 to the molecular layer, as  $\beta$  subunits are dependent on  $\alpha$  subunits for targeting to the plasma membrane (Gao et al., 1999). Therefore, performing immunohistochemistry for VDCC  $\beta$ 4 and ELKS1b/2 on P/Q-type VDCC knockout mice (*Cacna1a*<sup>-/-</sup>) allowed us to probe the potential *in vivo* interaction between VDCC  $\beta$ 4 and ELKS1. We measured the fluorescence intensity for both VDCC  $\beta$ 4 and ELKS1b/2 in the molecular layer and in the granule cell layer of *Cacna1a*<sup>-/-</sup> and wild-type littermates.

The signal intensity of VDCC  $\beta$ 4 decreased in the molecular layer of *Cacna1a*<sup>-/-</sup> cerebella (Fig. 3.6, left panels and 3.7A; wild-type:  $12.38 \pm 0.13$  mean fluorescence intensity in arbitrary units (A.U.); *Cacna1a*<sup>-/-</sup>:  $9.31 \pm 0.39$  A.U.,  $p = 0.02$ )(Billings et al., 2012). In contrast, there was no significant difference in VDCC  $\beta$ 4 in the granule cell layer (Fig. 3.6, left panels and 3.7C; wild-type:  $9.77 \pm 0.44$  A.U.; *Cacna1a*<sup>-/-</sup>:  $8.96 \pm 0.75$  A.U.,  $p = 0.23$ )(Billings et al., 2012). Additionally, Purkinje cell bodies appeared to have increased VDCC  $\beta$ 4 signal in the *Cacna1a*<sup>-/-</sup> (Fig 3.6)(Billings et al., 2012). The reduction in VDCC  $\beta$ 4 intensity in the molecular layer suggested that VDCC  $\beta$ 4 localization is perturbed by the loss of the  $\alpha$ 1A subunit.

However, ELKS1b/2 mean fluorescent intensity was unchanged in both the molecular layer (Fig. 3.6, right panels and 3.7B; wild-type:  $11.79 \pm 0.95$  A.U.;

*Cacna1a*<sup>-/-</sup>: 11.95 ± 0.82 A.U., p = 0.74)(Billings et al., 2012) and the granule cell layer (Fig 3.6, right panels and 3.7D; wild-type: 8.08 ± 1.00 A.U.; *Cacna1a*<sup>-/-</sup>: 8.14 ± 0.55 A.U. p = 0.95)(Billings et al., 2012) of *Cacna1a*<sup>-/-</sup> cerebella. These data suggest that ELKS1 is not dependent on VDCC β4 for trafficking into the molecular layer.

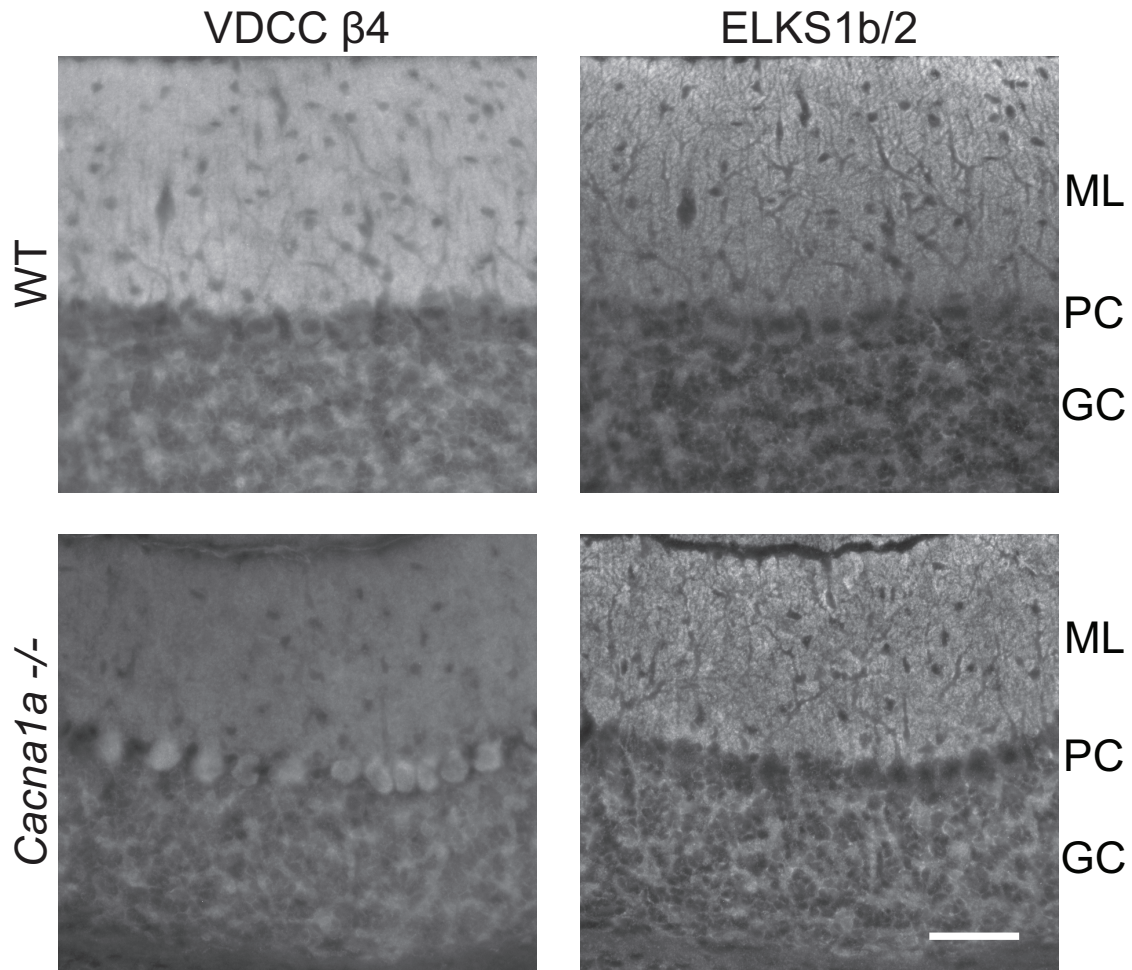


**Figure 3.6 VDCC  $\beta$ 4 signal is reduced in the molecular layer of *Cacna1a*<sup>-/-</sup> cerebellum.** Wild-type (WT) and *Cacna1a*<sup>-/-</sup> cerebella were stained for VDCC  $\beta$ 4 and ELKS1b/2 using fluorescent immunohistochemistry. The mean fluorescent intensity of VDCC  $\beta$ 4 decreased in the molecular layer (ML, left panels) but not the granule cell layer (GC, left panels) of *Cacna1a*<sup>-/-</sup> cerebellum at postnatal day 19 (n=3 animal pairs), whereas ELKS1b/2 showed no change (right panels). Purkinje cells (PC). Scale bar = 50  $\mu$ m. Figure adapted from (Billings et al., 2012).

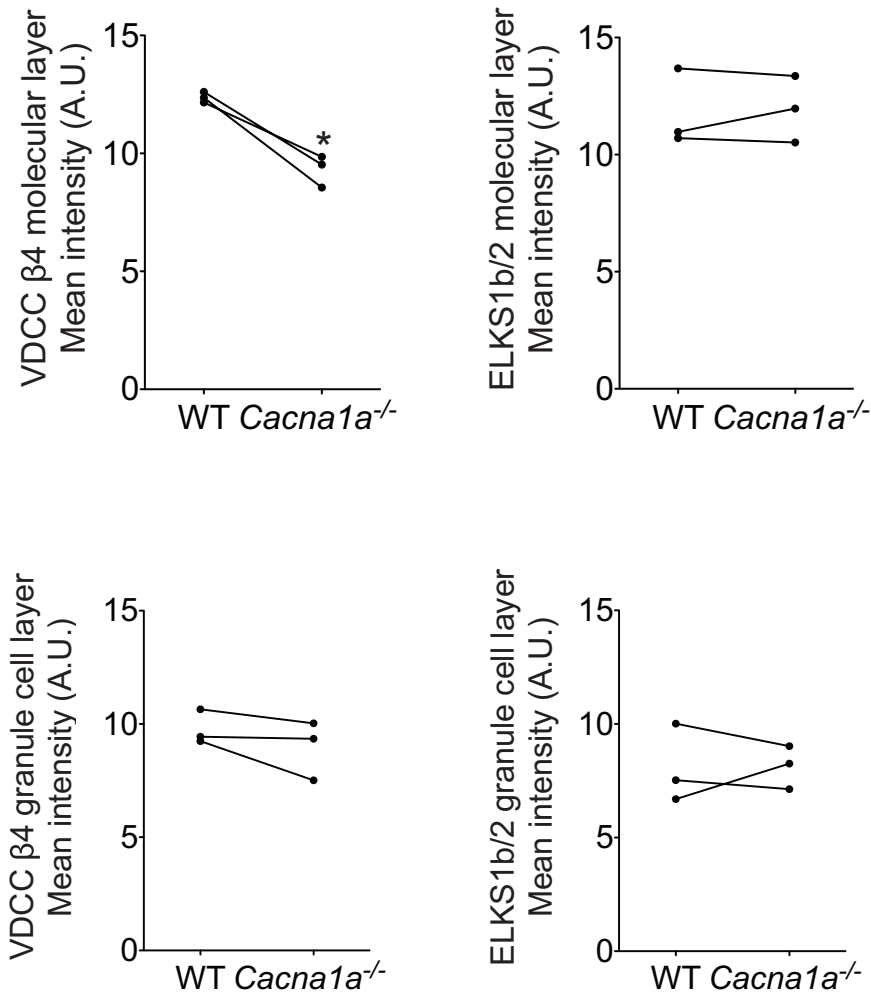


**Figure 3.7 Quantification of VDCC β4 and ELKS1 protein in the cerebellar cortex by immunohistochemistry.** VDCC β4 in the molecular layer was decreased in *Cacna1a*<sup>-/-</sup> (**A**), while ELKS1b/2 did not change (**B**). The signals for both proteins in the granule cell layers did not change between WT and *Cacna1a*<sup>-/-</sup> (**C**, **D**). The asterisk indicates a p-value < 0.05. Figure adapted from (Billings et al., 2012).

## 4. Discussion

VDCCs have an essential role in synaptic vesicle release (Catterall, 1998), and the CAZ has a very important role in regulating synaptic vesicle release and restricting it to the active zone (Rosenmund et al., 2003; Schoch and Gundelfinger, 2006). It therefore seems likely that these two components would need to be integrated together to accomplish spatially restricted, regulated and efficient synaptic vesicle release. However, our knowledge of the mechanisms and functions of interactions between the calcium and CAZ complexes remains incomplete. ELKS proteins are good candidates to mediate a connection between calcium channels and the CAZ because of their extensive intra-CAZ connections (Schoch and Gundelfinger, 2006).

In this study, we have investigated the possibility that ELKS and VDCC  $\beta$  proteins connect the calcium channel and CAZ complexes. We detected an interaction between ELKS2 and VDCC  $\beta$ 1b as well as between ELKS1b and VDCC  $\beta$ 4 by co-immunoprecipitation, showing that at least two isoforms of both ELKS and VDCC  $\beta$  proteins can interact. We observed moderate colocalization between ELKS1b and VDCC  $\beta$ 4 in the molecular layer of the cerebellum using fluorescent immunohistochemistry, suggesting that VDCC  $\beta$ 4 and ELKS1b interact in molecular layer synapses. These results represent a novel connection between calcium channel and CAZ complexes.

### **Interaction between VDCC and ELKS proteins**

We have shown that multiple isoforms of ELKS and VDCC  $\beta$  proteins are able to co-immunoprecipitate (Chen et al., 2011; Billings et al., 2012). These results are the first report of an interaction between ELKS and VDCC proteins in vertebrates. The fact that multiple isoforms can interact suggest that this interaction could be a mechanism that is present in many types of synapses, including both peripheral and central nervous system synapses.

The lack of association between the vertebrate ELKS2 and the VDCC  $\alpha$ 1A C-terminus (Chen et al., 2011) contrasts with the results from *Drosophila*, in which the ELKS homolog Bruchpilot binds to the C-terminus of the VDCC  $\alpha$  subunit Cac (Fouquet et al., 2009). This suggests that there are important differences in the organization of active zone proteins between *Drosophila* and vertebrates.

### **Colocalization between ELKS1 and VDCC $\beta$ 4 at molecular layer synapses**

In the molecular layer of the cerebellum, we observed that ELKS1 and VDCC  $\beta$ 4 puncta tended to reside next to each other, as shown by the high percentage of puncta that overlapped by 0.023 or 0.05  $\mu\text{m}^2$  (Billings et al., 2012). Some areas of overlap between ELKS1 and VDCC  $\beta$ 4 puncta could be found together with the synaptic marker Bassoon, suggesting that the two proteins colocalized at synapses. However, the overlap of the total area between VDCC  $\beta$ 4 and ELKS1b was moderate. One possible reason is that although ELKS1b localizes to the active zone and interacts with CAZ proteins (Wang et al., 2002; Deguchi-Tawarada et al., 2004; Inoue et al., 2006), it may be less tightly

associated to the CAZ than ELKS2 (Wang et al., 2002; Ko et al., 2006). In retina, ELKS1b is associated with the ribbon itself, where as ELKS2 is found at the base of the ribbon, much closer to the active zone membrane (Deguchi-Tawarada et al., 2006), suggesting that ELKS1b is not as closely associated with the site of vesicle fusion.

### ***Cacna1a*<sup>-/-</sup> mouse analysis**

In order to further probe the relationship between VDCC  $\beta$ 4 and ELKS1, we performed immunohistochemistry for VDCC  $\beta$ 4 and ELKS1b on cerebella of *Cacna1a*<sup>-/-</sup> mice. We found that the signal intensity of VDCC  $\beta$ 4 in the molecular layer decreased (Billings et al., 2012). This is the first report of a defect in the amount of VDCC  $\beta$ 4 in the molecular layer in *Cacna1a*<sup>-/-</sup> mice. This could be due to less transport of VDCC  $\beta$ 4 into the molecular layer, because VDCC  $\beta$  subunits are dependent on VDCC  $\alpha$  subunits for normal plasma membrane targeting (Gao et al., 1999). The reduction of VDCC  $\beta$ 4 in the molecular layer in spite of the expression of other VDCC  $\alpha$  subunits in the cerebellum (Ludwig et al., 1997; Jun et al., 1999) suggests a specific interaction between VDCC  $\alpha$ 1A and  $\beta$ 4 subunits that cannot be compensated for by other VDCC  $\alpha$  subunits.

While VDCC  $\beta$ 4 signal decreased in the molecular layer in *Cacna1a*<sup>-/-</sup> mice, ELKS1b signal was not changed, suggesting that ELKS1b does not rely on VDCC  $\beta$ 4 for trafficking into the molecular layer (Billings et al., 2012). However, the interactions between ELKS1b and other synaptic proteins may stabilize ELKS1b at the active zone in the absence of VDCC  $\beta$ 4. Similarly, liprin- $\alpha$ , which

interacts directly with ELKS2 $\alpha$  as well as many other synaptic proteins (Schoch and Gundelfinger, 2006), does not decrease in the synaptosomal fraction in ELKS2 $\alpha$  knockout mice (Kaesler et al., 2009), showing that the loss of a single interaction partner was not sufficient to change the localization of liprin- $\alpha$ .

The *Cacna1a*<sup>-/-</sup> mouse NMJ was investigated previously, and the number of Bassoon puncta (by light microscopy) and the number of active zones (by electron microscopy) were decreased compared to wild-type (Nishimune et al., 2004). Further work using a mouse model that lacked both P/Q- and N-type VDCC (Double knockout (DKO); *Cacna1a*<sup>-/-</sup> *Cacna1b*<sup>-/-</sup>) revealed an even stronger decrease in Bassoon signal, and also showed that Piccolo and ELKS signals were reduced at DKO NMJs (Chen et al., 2011). These data led us to postulate that the calcium channel has a central role in the organization of the active zone.

As this important role of the calcium channel might be conserved among different types of synapses, we hypothesized that we would see a similar decrease in the amount of CAZ proteins in the cerebellum of *Cacna1a*<sup>-/-</sup> mice. However, ELKS1b/2 protein intensity did not change (Billings et al., 2012). This discrepancy between the results from the NMJ and the cerebellum could be due to a different degree of reliance on the P/Q-type VDCC for synaptic transmission. The parallel fibers of the cerebellum rely on multiple VDCC  $\alpha$  subunits to carry their evoked calcium current (Mintz et al., 1995), whereas the mature NMJ relies exclusively on the P/Q-type calcium channel (Rosato Siri and Uchitel, 1999). The

active zone proteins at the NMJ might therefore be more sensitive to the loss of P/Q-type VDCC than those in the parallel fiber synapses.

## 5. Conclusions

The findings demonstrated interactions between ELKS proteins and VDCC  $\beta$  subunits. Isoforms expressed in motor neurons (VDCC  $\beta$ 1b and ELKS2) as well as those preferentially expressed in cerebellum (VDCC  $\beta$ 4 and ELKS1b) were both found to co-immunoprecipitate. Furthermore, VDCC  $\beta$ 4 and ELKS1b colocalized moderately at synapses in the molecular layer of the cerebellum, suggesting a synaptic function for a VDCC  $\beta$ 4-ELKS1b interaction, such as linking VDCCs to the CAZ.

We also showed for the first time that the loss of VDCC  $\alpha$ 1A affects VDCC  $\beta$ 4 protein localization *in vivo*, supporting *in vitro* and cell culture model reports that VDCC  $\beta$  subunits require VDCC  $\alpha$  subunits for trafficking (Gao et al., 1999; Bichet et al., 2000; Obermair et al., 2010).

Overall, our study describes novel interactions between ELKS and VDCC  $\beta$  subunits that may contribute to active zone organization by linking calcium channels to the CAZ.

## 6. References

Allen Mouse Brain Atlas [Internet]. Seattle (WA): Allen Institute for Brain Science. ©2009. Available from: <http://mouse.brain-map.org>

Bichet, D., V. Cornet, S. Geib, E. Carlier, S. Volsen, T. Hoshi, Y. Mori, and M. De Waard. 2000. The I-II loop of the Ca<sup>2+</sup> channel alpha1 subunit contains an endoplasmic reticulum retention signal antagonized by the beta subunit. *Neuron*. 25:177-190.

Billings, S.E., G.L. Clarke, and H. Nishimune. 2012. ELKS1 and Ca<sup>2+</sup> channel subunit  $\beta$ 4 interact and colocalize at cerebellar synapses. *Neuroreport*. 23:49-54.

Black, J.L., 3rd. 2003. The voltage-gated calcium channel gamma subunits: a review of the literature. *J Bioenerg Biomembr*. 35:649-660.

Bolte, S., and F.P. Cordelieres. 2006. A guided tour into subcellular colocalization analysis in light microscopy. *J Microsc*. 224:213-232.

Catterall, W.A. 1998. Structure and function of neuronal Ca<sup>2+</sup> channels and their role in neurotransmitter release. *Cell Calcium*. 24:307-323.

Catterall, W.A. 2000. Structure and regulation of voltage-gated Ca<sup>2+</sup> channels. *Annu Rev Cell Dev Biol*. 16:521-555.

Chen, J., S.E. Billings, and H. Nishimune. 2011. Calcium channels link the muscle-derived synapse organizer laminin beta2 to Bassoon and CAST/Erc2 to organize presynaptic active zones. *J Neurosci*. 31:512-525.

Coppola, T., S. Magnin-Luthi, V. Perret-Menoud, S. Gattesco, G. Schiavo, and R. Regazzi. 2001. Direct interaction of the Rab3 effector RIM with Ca<sup>2+</sup> channels, SNAP-25, and synaptotagmin. *J Biol Chem*. 276:32756-32762.

De Waard, M., D.R. Witcher, M. Pragnell, H. Liu, and K.P. Campbell. 1995. Properties of the alpha 1-beta anchoring site in voltage-dependent Ca<sup>2+</sup> channels. *J Biol Chem*. 270:12056-12064.

Deguchi-Tawarada, M., E. Inoue, E. Takao-Rikitsu, M. Inoue, I. Kitajima, T. Ohtsuka, and Y. Takai. 2006. Active zone protein CAST is a component of conventional and ribbon synapses in mouse retina. *J Comp Neurol*. 495:480-496.

Deguchi-Tawarada, M., E. Inoue, E. Takao-Rikitsu, M. Inoue, T. Ohtsuka, and Y. Takai. 2004. CAST2: identification and characterization of a protein structurally related to the presynaptic cytomatrix protein CAST. *Genes Cells*. 9:15-23.

Eroglu, C., N.J. Allen, M.W. Susman, N.A. O'Rourke, C.Y. Park, E. Ozkan, C. Chakraborty, S.B. Mulinyawe, D.S. Annis, A.D. Huberman, E.M. Green, J. Lawler, R. Dolmetsch, K.C. Garcia, S.J. Smith, Z.D. Luo, A. Rosenthal, D.F. Mosher, and B.A. Barres. 2009. Gabapentin receptor alpha2delta-1 is a neuronal thrombospondin receptor responsible for excitatory CNS synaptogenesis. *Cell*. 139:380-392.

Fish, K.N., R.A. Sweet, A.J. Deo, and D.A. Lewis. 2008. An automated segmentation methodology for quantifying immunoreactive puncta number and fluorescence intensity in tissue sections. *Brain Research*. 1240:62-72.

Fouquet, W., D. Oswald, C. Wichmann, S. Mertel, H. Depner, M. Dyba, S. Hallermann, R.J. Kittel, S. Eimer, and S.J. Sigrist. 2009. Maturation of active zone assembly by *Drosophila* Bruchpilot. *J Cell Biol*. 186:129-145.

Gao, T., A.J. Chien, and M.M. Hosey. 1999. Complexes of the alpha1C and beta subunits generate the necessary signal for membrane targeting of class C L-type calcium channels. *J Biol Chem*. 274:2137-2144.

Grigoriev, I., K.L. Yu, E. Martinez-Sanchez, A. Serra-Marques, I. Smal, E. Meijering, J. Demmers, J. Peranen, R.J. Pasterkamp, P. van der Sluijs, C.C. Hoogenraad, and A. Akhmanova. 2011. Rab6, Rab8, and MICAL3 cooperate in controlling docking and fusion of exocytotic carriers. *Curr Biol*. 21:967-974.

Hida, Y., and T. Ohtsuka. 2010. CAST and ELKS proteins: structural and functional determinants of the presynaptic active zone. *J Biochem*. 148:131-137.

Inoue, E., M. Deguchi-Tawarada, E. Takao-Rikitsu, M. Inoue, I. Kitajima, T. Ohtsuka, and Y. Takai. 2006. ELKS, a protein structurally related to the active zone protein CAST, is involved in Ca<sup>2+</sup>-dependent exocytosis from PC12 cells. *Genes Cells*. 11:659-672.

Jun, K., E.S. Piedras-Renteria, S.M. Smith, D.B. Wheeler, S.B. Lee, T.G. Lee, H. Chin, M.E. Adams, R.H. Scheller, R.W. Tsien, and H.S. Shin. 1999. Ablation of P/Q-type Ca(2+) channel currents, altered synaptic transmission, and progressive ataxia in mice lacking the alpha(1A)-subunit. *Proc Natl Acad Sci U S A*. 96:15245-15250.

Juranek, J., K. Mukherjee, M. Rickmann, H. Martens, J. Calka, T.C. Sudhof, and R. Jahn. 2006. Differential expression of active zone proteins in neuromuscular junctions suggests functional diversification. *Eur J Neurosci*. 24:3043-3052.

Kaesler, P.S., L. Deng, A.E. Chavez, X. Liu, P.E. Castillo, and T.C. Sudhof. 2009. ELKS2alpha/CAST deletion selectively increases neurotransmitter release at inhibitory synapses. *Neuron*. 64:227-239.

Kaesler, P.S., L. Deng, Y. Wang, I. Dulubova, X. Liu, J. Rizo, and T.C. Sudhof. 2011. RIM proteins tether Ca<sup>2+</sup> channels to presynaptic active zones via a direct PDZ-domain interaction. *Cell*. 144:282-295.

Katz, B. 1996. Neural transmitter release: from quantal secretion to exocytosis and beyond. The Fenn Lecture. *J Neurocytol*. 25:677-686.

Kiyonaka, S., M. Wakamori, T. Miki, Y. Uriu, M. Nonaka, H. Bito, A.M. Beedle, E. Mori, Y. Hara, M. De Waard, M. Kanagawa, M. Itakura, M. Takahashi, K.P. Campbell, and Y. Mori. 2007. RIM1 confers sustained activity and neurotransmitter vesicle anchoring to presynaptic Ca<sup>2+</sup> channels. *Nat Neurosci*. 10:691-701.

Ko, J., C. Yoon, G. Piccoli, H.S. Chung, K. Kim, J.R. Lee, H.W. Lee, H. Kim, C. Sala, and E. Kim. 2006. Organization of the presynaptic active zone by ERC2/CAST1-dependent clustering of the tandem PDZ protein syntenin-1. *J Neurosci*. 26:963-970.

Kurshan, P.T., A. Oztan, and T.L. Schwarz. 2009. Presynaptic alpha2delta-3 is required for synaptic morphogenesis independent of its Ca<sup>2+</sup>-channel functions. *Nat Neurosci*. 12:1415-1423.

Landis, D.M., A.K. Hall, L.A. Weinstein, and T.S. Reese. 1988. The organization of cytoplasm at the presynaptic active zone of a central nervous system synapse. *Neuron*. 1:201-209.

Leitch, B., O. Shevtsova, D. Guevremont, and J. Williams. 2009. Loss of calcium channels in the cerebellum of the ataxic and epileptic stargazer mutant mouse. *Brain Res*. 1279:156-167.

Ludwig, A., V. Flockerzi, and F. Hofmann. 1997. Regional expression and cellular localization of the alpha1 and beta subunit of high voltage-activated calcium channels in rat brain. *J Neurosci*. 17:1339-1349.

Mintz, I.M., B.L. Sabatini, and W.G. Regehr. 1995. Calcium control of transmitter release at a cerebellar synapse. *Neuron*. 15:675-688.

Mishchenko, Y. 2010. On optical detection of densely labeled synapses in neuropil and mapping connectivity with combinatorially multiplexed fluorescent synaptic markers. *PLoS One*. 5:e8853.

Monier, S., F. Jollivet, I. Janoueix-Lerosey, L. Johannes, and B. Goud. 2002. Characterization of novel Rab6-interacting proteins involved in endosome-to-TGN transport. *Traffic*. 3:289-297.

Muller, C.S., A. Haupt, W. Bildl, J. Schindler, H.G. Knaus, M. Meissner, B. Rammner, J. Striessnig, V. Flockerzi, B. Fakler, and U. Schulte. 2010.

Quantitative proteomics of the Cav2 channel nano-environments in the mammalian brain. *Proc Natl Acad Sci U S A*. 107:14950-14957.

Nakata, T., T. Yokota, M. Emi, and S. Minami. 2002. Differential expression of multiple isoforms of the ELKS mRNAs involved in a papillary thyroid carcinoma. *Genes Chromosomes Cancer*. 35:30-37.

Neher, E. 1998. Vesicle pools and Ca<sup>2+</sup> microdomains: new tools for understanding their roles in neurotransmitter release. *Neuron*. 20:389-399.

Nishimune, H., J.R. Sanes, and S.S. Carlson. 2004. A synaptic laminin-calcium channel interaction organizes active zones in motor nerve terminals. *Nature*. 432:580-587.

Obermair, G.J., B. Schlick, V. Di Biase, P. Subramanyam, M. Gebhart, S. Baumgartner, and B.E. Flucher. 2010. Reciprocal interactions regulate targeting of calcium channel beta subunits and membrane expression of alpha1 subunits in cultured hippocampal neurons. *J Biol Chem*. 285:5776-5791.

Ohara-Imaizumi, M., T. Ohtsuka, S. Matsushima, Y. Akimoto, C. Nishiwaki, Y. Nakamichi, T. Kikuta, S. Nagai, H. Kawakami, T. Watanabe, and S. Nagamatsu. 2005. ELKS, a protein structurally related to the active zone-associated protein CAST, is expressed in pancreatic beta cells and functions in insulin exocytosis: interaction of ELKS with exocytotic machinery analyzed by total internal reflection fluorescence microscopy. *Mol Biol Cell*. 16:3289-3300.

Ohtsuka, T., E. Takao-Rikitsu, E. Inoue, M. Inoue, M. Takeuchi, K. Matsubara, M. Deguchi-Tawarada, K. Satoh, K. Morimoto, H. Nakanishi, and Y. Takai. 2002. Cast: a novel protein of the cytomatrix at the active zone of synapses that forms a ternary complex with RIM1 and munc13-1. *J Cell Biol*. 158:577-590.

Pagani, R., M. Song, M. McEnery, N. Qin, R.W. Tsien, L. Toro, E. Stefani, and O.D. Uchitel. 2004. Differential expression of alpha 1 and beta subunits of voltage dependent Ca<sup>2+</sup> channel at the neuromuscular junction of normal and P/Q Ca<sup>2+</sup> channel knockout mouse. *Neuroscience*. 123:75-85.

Palay, S., and V. Chan-Palay. 1974. Cerebellar cortex: cytology and organization. Springer, New York. pp. 63-99.

Rosato Siri, M.D., and O.D. Uchitel. 1999. Calcium channels coupled to neurotransmitter release at neonatal rat neuromuscular junctions. *J Physiol*. 514 ( Pt 2):533-540.

Rosenmund, C., J. Rettig, and N. Brose. 2003. Molecular mechanisms of active zone function. *Curr Opin Neurobiol*. 13:509-519.

Schoch, S., and E.D. Gundelfinger. 2006. Molecular organization of the presynaptic active zone. *Cell Tissue Res*. 326:379-391.

Scott, V.E., M. De Waard, H. Liu, C.A. Gurnett, D.P. Venzke, V.A. Lennon, and K.P. Campbell. 1996. Beta subunit heterogeneity in N-type Ca<sup>2+</sup> channels. *J Biol Chem.* 271:3207-3212.

Shibasaki, T., Y. Sunaga, K. Fujimoto, Y. Kashima, and S. Seino. 2004. Interaction of ATP sensor, cAMP sensor, Ca<sup>2+</sup> sensor, and voltage-dependent Ca<sup>2+</sup> channel in insulin granule exocytosis. *J Biol Chem.* 279:7956-7961.

Stanley, E.F. 1997. The calcium channel and the organization of the presynaptic transmitter release face. *Trends Neurosci.* 20:404-409.

Sudhof, T.C. 2008. Generation of an Erc1 knock-out mouse. Mouse Genome Informatics. MGI: 3784842.

Takao-Rikitsu, E., S. Mochida, E. Inoue, M. Deguchi-Tawarada, M. Inoue, T. Ohtsuka, and Y. Takai. 2004. Physical and functional interaction of the active zone proteins, CAST, RIM1, and Bassoon, in neurotransmitter release. *J Cell Biol.* 164:301-311.

Takeuchi, T., T. Miyazaki, M. Watanabe, H. Mori, K. Sakimura, and M. Mishina. 2005. Control of synaptic connection by glutamate receptor delta2 in the adult cerebellum. *J Neurosci.* 25:2146-2156.

Tao-Cheng, J.H. 2007. Ultrastructural localization of active zone and synaptic vesicle proteins in a preassembled multi-vesicle transport aggregate. *Neuroscience.* 150:575-584.

Uriu, Y., S. Kiyonaka, T. Miki, M. Yagi, S. Akiyama, E. Mori, A. Nakao, A.M. Beedle, K.P. Campbell, M. Wakamori, and Y. Mori. 2010. Rab3-interacting molecule gamma isoforms lacking the Rab3-binding domain induce long lasting currents but block neurotransmitter vesicle anchoring in voltage-dependent P/Q-type Ca<sup>2+</sup> channels. *J Biol Chem.* 285:21750-21767.

Walker, D., D. Bichet, K.P. Campbell, and M. De Waard. 1998. A beta 4 isoform-specific interaction site in the carboxyl-terminal region of the voltage-dependent Ca<sup>2+</sup> channel alpha 1A subunit. *J Biol Chem.* 273:2361-2367.

Walker, D., D. Bichet, S. Geib, E. Mori, V. Cornet, T.P. Snutch, Y. Mori, and M. De Waard. 1999. A new beta subtype-specific interaction in alpha1A subunit controls P/Q-type Ca<sup>2+</sup> channel activation. *J Biol Chem.* 274:12383-12390.

Wang, Y., X. Liu, T. Biederer, and T.C. Sudhof. 2002. A family of RIM-binding proteins regulated by alternative splicing: Implications for the genesis of synaptic active zones. *Proc Natl Acad Sci U S A.* 99:14464-14469.

Zhai, R., G. Olias, W.J. Chung, R.A. Lester, S. tom Dieck, K. Langnaese, M.R. Kreutz, S. Kindler, E.D. Gundelfinger, and C.C. Garner. 2000. Temporal

appearance of the presynaptic cytomatrix protein bassoon during synaptogenesis. *Mol Cell Neurosci.* 15:417-428.

## 7. Appendix

This thesis contains figures and text from the following publications:

Billings, S.E., G.L. Clarke, and H. Nishimune. 2012. ELKS1 and Ca<sup>2+</sup> channel subunit  $\beta$ 4 interact and colocalize at cerebellar synapses. *Neuroreport*. 23:49-54.

Chen, J., S.E. Billings, and H. Nishimune. 2011. Calcium channels link the muscle-derived synapse organizer laminin beta2 to Bassoon and CAST/Erc2 to organize presynaptic active zones. *J Neurosci*. 31:512-525.